# High-Resolution Electrohydrodynamic Jet Printing of Molten Polycaprolactone

Patrick M. Sammons, Kira Barton

University of Michigan, Ann Arbor, MI 48109
Mechanical Engineering Department

## Abstract

Polycaprolactone (PCL) is a biocompatible and biodegradable polymer that is commonly used in drug delivery systems, medical structures, and tissue engineering applications. Typical additive manufacturing methods of PCL structures for tissue engineering applications either require harsh organic solvents or are only capable of producing relatively large feature sizes, which are not compatible with some of the desired applications. Electrohydrodynamic jet (e-jet) printing, an additive manufacturing process which uses an electric field to induce jetting from a microcapillary nozzle, is an attractive method for producing PCL tissue engineering structures due to the achievable resolution and the ability to print highly viscous inks. In this work, experimental investigation into the ability to print pure, molten PCL using the e-jet process is carried out. A characterization of the process inputs that yield suitable printing regimes is presented. Demonstration of the achievable resolution with e-jet printing is presented in the form of printed, high-resolution structures.

## Introduction

The application of biocompatible, biodegradable, and bioresorbable materials for drug delivery [8], medical devices [9], and tissue engineering applications [10] is garnering increased attention. A popular subclass of these materials are polymers [1] which include polylactide (PLA), polycaprolactone (PCL), polyethylene glycol (PEG), in additions to many others. In particular, PCL has found numerous applications in tissue engineering applications due to its relatively low tensile strength, high elongation at breakage, and processability.

For tissue engineering applications, inkjet and electrospinning (e-spinning) of PCL is popular. In inkjet, because it is solid at room temperature and its viscosity when molten, PCL is typically carried with a solvent in order to enable printing [13]. However, these solvents can be harmful or the resulting PCL structure after the solvent has been removed does not display desirable properties [13]. Alternatively, e-spinning can be used to manufacture large structures comprised of small fiber elements using pure PCL [11]. The major disadvantage of the e-spinning process stems from the unpredictable behavior of the filament produced. It is therefore difficult to control the placement of these fibers which in turn limits the minimum feature size that can be successfully created with e-spinning. Further, there are a number of tissue engineering applications where it is advantageous to precisely place material and to create fine features. Therefore, alternative methods for processing of PCL should be considered.

Electrohydrodynamic jet (e-jet) printing is an emerging micro-/nano-scale additive manufacturing (AM) process that shows promise for a variety of applications [12] including the manufacture of conformal, printed electronics and biomedical structures. In e-jet printing, a voltage is applied between an ink-filled emitter and an attractor (typically a charged conductive microcapillary nozzle and a grounded conductive substrate, respectively). The electric field formed by the voltage potential induces an electric stress in the ink and causes a bulk deformation. At a critical

level of the electric field, the electric stress overcomes restorative surface tension stresses in the ink and a discrete volume of fluid is ejected from the emitter towards the attractor. By adjusting the magnitude and duration of the electric field formed by the voltage potential, micro- and nano-sized droplets can be created on a variety of substrates. While the underlying physics of both the e-jet and e-spinning processes are similar, the two processes differ in several ways. First, e-jet printing is performed with the nozzle relatively close ($\sim$3-10 times the nozzle diameter in e-jet printing versus $\sim$100 times the nozzle diameter in e-spinning) to the substrate. This enables finer control of the placement of material on the substrate. Secondly, e-jet printing is operated in a "stop-start" manner where the voltage is modulated throughout the course of a build to fabricate features. This is in contrast to e-spinning where the voltage is held constant and the filament produced in e-spinning is continuously collected, typically on a mandrel. Figure 1 provides a schematic comparing the two processes. In e-jet printing, the ejection of material is periodic in time either by modulating the voltage ("Pulse") or by operating in a regime where the jetting is intermittent and caused by a persistent high voltage ("DC"). E-spinning is a constant process in terms of both the applied voltage and the material flow.

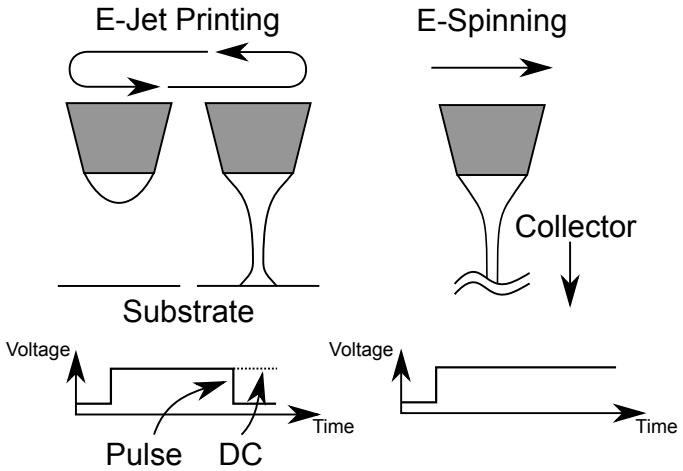


**Figure 1: Schematic of the e-jet and e-spinning processes with characteristic voltage signals.**

The rest of the paper is structured as follows. First, a description of the experimental system used to e-jet print molten PCL is given, including properties of PCL. Then, characteristics of the observed printing behavior is discussed. Finally, a summary, conclusion, and a discussion of future work is given.

## Experimental System Description

In this section, details of the physical experimental system are given. Then, material properties of the PCL used here are given. Finally, details regarding the expected limiting behavior while printing molten PCL are given.

### *A. E-Jet Printer Description*

The e-jet printer used in this work is a custom built system developed within the Barton Research Group. The e-jet printer is comprised of a motion system, a print head, and a set of auxiliary components. The motion system consists of two stacked Aerotech stages (ATS15020-

1-02B) to enable X-Y motion with a vertical Z-axis mounted adjacent to the X-Y stage to enable vertical positioning. The horizontal stages are each repeatable to $\pm$ 2 $\mu$m

The print head consists of an in-house machined aluminum body into which a heating element and a syringe barrel can be inserted. The heating element is utilized with an external controller (Omron E5C2) and temperature feedback measured using a thermocouple attached to the aluminum body. To the syringe barrel, which contains the material to be printed, a custom fabricated nozzle is attached. The nozzle consists of tungsten filament 35 gauge blunt needle (WPI NF35BL) inserted into a shortened 15 gauge blunt stainless steel needle. The print head is mounted to the Z-axis.

There are three auxiliary systems integrated into the e-jet printer: a video camera, a high voltage amplifier, and an air pressure regulator. The video camera (Lumenera Infinity 2) is a color 2.0 Megapixel USB camera used to monitor the e-jet printing process. In line with the monitoring camera is a set of optics to provide magnification. The voltage amplifier (Ultravolt/Advanced Energy HVA Series) produces up to 2 kV to the nozzle. Finally, the pressure regulator is capable of 1 PSI resolution at a minimum of 5 PSI. The staging, the pressure regulator, and the voltage amplifier are controlled via a LabVIEW interface. Monitoring via the camera is enabled using software provided by the manufacturer. Figure 2 shows a schematic of the e-jet printer with the above components and systems labeled.

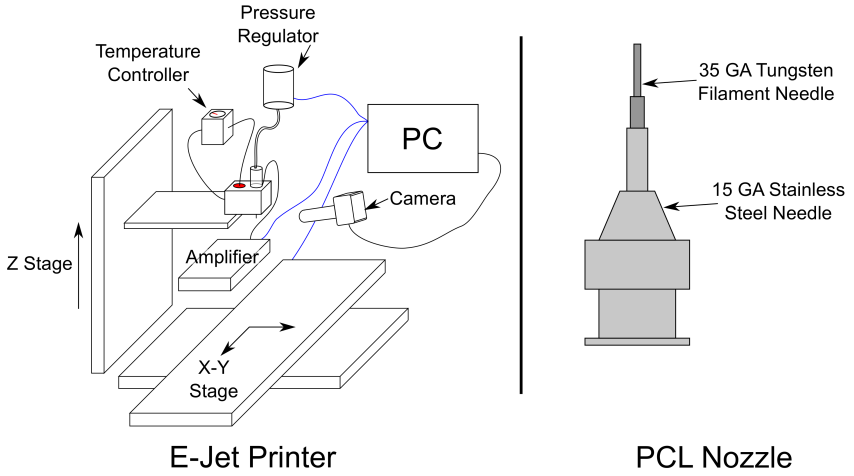


**Figure 2: Schematic of the e-jet printer used in this work with relevant components and subsystems labeled (left) and a schematic of the custom nozzle fabricated for printing molten PCL (right).**

*B. Polycaprolactone Material and Jetting Properties*

Selected relevant material properties of molten PCL are listed in Table 1 along with those of deionized (DI) water for comparison. Sigma-Aldrich polycaprolactone average weight number Mn = 45,000 is used for this work. The most noticeable difference between these two materials is viscosity. Molten PCL is approximately $1 \times 10^6$ more viscous than DI water, but possess similar electrical and surface tension properties.

There are several unique challenges associated with attempting to print pure PCL. First, at room temperature, PCL is solid. Therefore, typical methods for printing PCL use one of several

**Table 1: Material properties of molten PCL and room temperature DI water.**

| | Material | |
|---|---|---|
| **Property** | **PCL** | **DI Water** |
| Viscosity, $\mu$ (Pa-s) | $\sim 10 \times 10^3$ [7] | $1.0 \times 10^{-3}$ |
| Surface Tension Coefficient, $\gamma$ (N/m) | $\sim 45 \times 10^{-3}$ [4] | $72.8 \times 10^{-3}$ |
| Density, $\rho$ (kg/m$^3$) | 1145 | 998 |
| Conductivity, $\sigma$ (S/m) | $2.6 \times 10^{-5}$ [3] | 0.1-5$\times 10^{-5}$ |
| Relative Permittivity, $\epsilon_r$ | 3.5-4.5 [5] | $\sim$80 |

solvents. Secondly, when molten, PCL is relatively viscous. This is a significant issue for systems such as inkjet and aerosol jet which possess an upper limit on ink viscosity well below that of molten PCL. Additionally, because molten PCL has a high viscosity, the time constant of the jetting behavior is governed by viscosity rather than surface tension.

To understand the limiting behavior in the e-jet printing of molten PCL, consider the following time scales. The capillary time scale of the process through a 150 $\mu$m nozzle, defined as [6]

$$\tau_c = \sqrt{\frac{\rho L^3}{\gamma}} \tag{1}$$

where $\tau_c$ is the capillary time scale (s), $\rho$ is the ink density (kg/m$^3$), $L$ is the characteristic length (m) taken here as the nozzle inner diameter, and $\gamma$ is the ink surface tension coefficient (N/m), is $\tau_c = 2.93 \times 10^{-4}$ s. Compare this value with that of DI water, $\tau_c = 2.12 \times 10^{-4}$ s. Alternatively, the viscous flow time scale for a system with the same nozzle size, defined as [2],

$$\tau_\mu = \frac{\rho L^2}{\mu} \tag{2}$$

where $\tau_\mu$ is the viscous flow time scale (s) and $\mu$ is the ink viscosity (Pa-s), is $\tau_\mu = 2.58 \times 10^{-8}$ s for molten PCL and $\tau_\mu = 2.25 \times 10^{-2}$ s for DI water. The viscous flow time scale for molten PCL, where smaller time scales indicate greater importance in the flow, dominates that of water. This is expected given the disparity in viscosity between the two fluids.

A significant deviation of the behavior of molten PCL over typical inks in e-jet printing can be observed by further examining the charge relaxation time,

$$\tau_e = \frac{\epsilon}{\sigma} \tag{3}$$

where $\tau_e$ is the charge relaxation time and an indicator of the importance of the charge density movement in the fluid (s), $\sigma$ is the fluid conductivity (S/m), and $\epsilon$ is the fluid permittivity (F/m). For molten PCL, the charge relaxation time scale is $\tau_e = 1.02 \times 10^{-6}$ s while that of DI water is $\tau_e = 3.54 \times 10^{-5}$ s. In context, it can be seen that the viscous flow scale significantly dominates the other two time scales for PCL while the charge relaxation time scale dominates for DI water. However, there exists more parity in the time scales for DI water than for PCL.

From the above analysis it can be expected that the jetting behavior and flow of molten PCL will be limited by viscous flow and that the jetting will happen over a longer time span than inks with similar material properties but lower viscosity.

## E-Jet Printing Characterization

In order to characterize the jetting ability of molten PCL in the experimental setup described above, a series of tests are performed using pulse printing (see Figure 1). During the exploration of this regime, evidence of a regime where DC printing results in intermittent jetting was discovered. Details regarding this behavior are given in the second subsection. Table 2 provides the experimental parameters used for all of the experiments detailed here.

**Table 2: Process parameters for e-jet printing characterization of PCL**

| Parameter | Value |
|---|---|
| Standoff distance, $d_N$ ($\mu$m) | 100 |
| Temperature set point, $T_s$ (C) | 90 |
| X-axis pitch, $p_x$ ($\mu$m) | 50 |
| Y-axis pitch, $p_y$ ($\mu$m) | 100 |
| Nozzle outer radius at outlet, $r_N$ ($\mu$m) | 67.5 |
| Back pressure, $P_0$ (PSI) | 0 |

### *C. Pulse Printing*

In this section, details regarding the size of features produced using a select range of voltages and pulse widths will be presented. Table 3 gives the parameter levels tested here. The parameters presented in Table 3 were initially determined by exploring the voltage-pulse width space and noting the boundaries where the fluid forms a distinct cone and successfully deposited material on the substrate.

**Table 3: Experimental levels used for characterizing PCL pulse printing**

| | Level | | |
|---|---|---|---|
| **Parameter** | **High** | **Mid** | **Low** |
| High Voltage (V) | 1000 | 850 | 750 |
| Pulse Width (ms) | {1500,2000,2500} | {3000,2500,2000} | {3500,4000,4500} |

Table 4 provides a summary of the Feret diameter, i.e., the largest dimension across the structure, statistics for each of the experimental conditions. Figures 3 through 4 give histograms and normal distribution fits for selected data sets. Examining the results in Table 4 and the selected results in the provided figures, it can be observed that the droplet diameter is approximately constant across the tested voltages and pulse widths. Further, while the mean values of diameter are all extremely close, the standard deviation for all of the tested combinations, with the exception of the final 750 V trial, are less than 20% of the mean. This indicates very repeatable behavior.

Figure 5 summarizes the trends of the measured Feret diameter with respect to pulse width and voltage. As stated above, the printing behavior appears insensitive to changes in pulse width and voltage. While this is initially a surprising result, in the context of the time scales presented above, it is an expected result as the PCL behavior is dominated by the viscous flow time scale rather than charge relaxation which is typically the case in e-jet printing.

**Table 4: Summary of pulse printing results.**

| Experimental Condition | Mean ($\mu$m) | Std. Dev. ($\mu$m) |
|---|---|---|
| 1000 V, 1500 ms | 20.02 | 3.82 |
| 1000 V, 2000 ms | 28.00 | 2.78 |
| 1000 V, 2500 ms | 23.53 | 2.03 |
| 1000 V, 1500 ms | 20.02 | 3.82 |
| 850 V, 2500 ms | 22.77 | 3.25 |
| 850 V, 3500 ms | 23.42 | 3.20 |
| 750 V, 4000 ms | 23.73 | 4.35 |
| 750 V, 4500 ms | 22.27 | 6.72 |

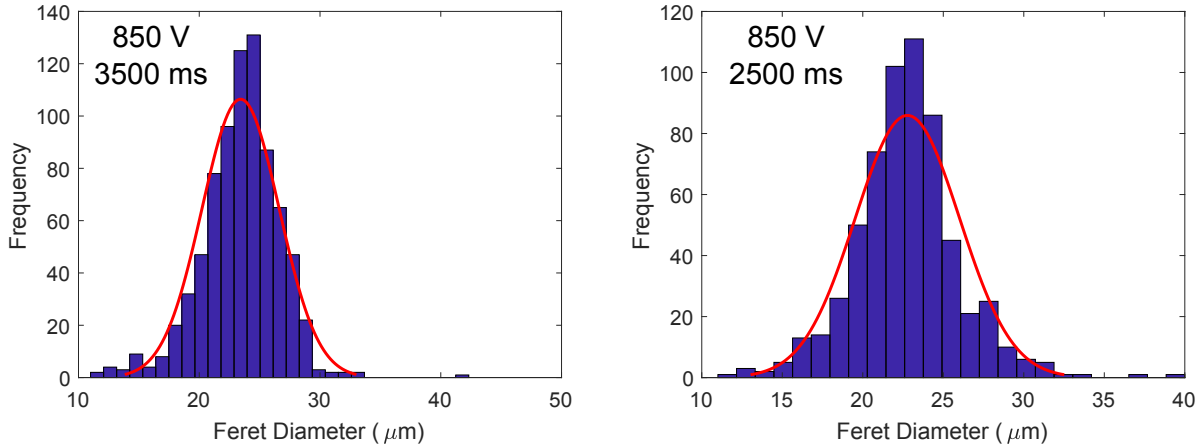


**Figure 3: Feret diameter histogram and normal distribution fit for 850 V and 3500 ms pulse width (left) and 850 V and 2500 ms pulse width (right).**

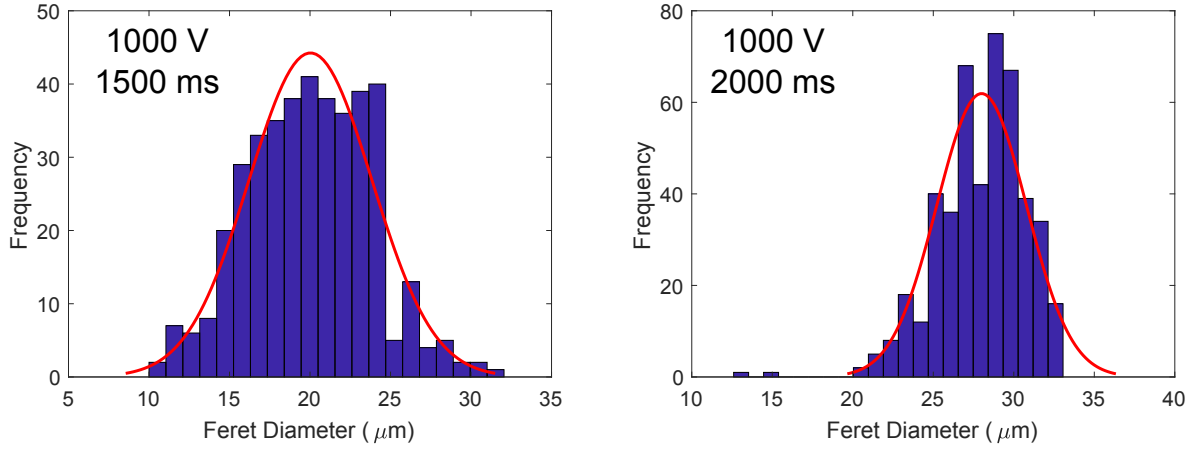


**Figure 4: Feret diameter histogram and normal distribution fit for 1000 V and 2000 ms pulse width (left) and 1000 V and 1500 ms pulse width (right).**

*D. DC Printing*

While exploring the voltage-pulse width parameter space, intermittent jetting was observed while voltage was high. This is a previously unreported behavior for inks as viscous as PCL.

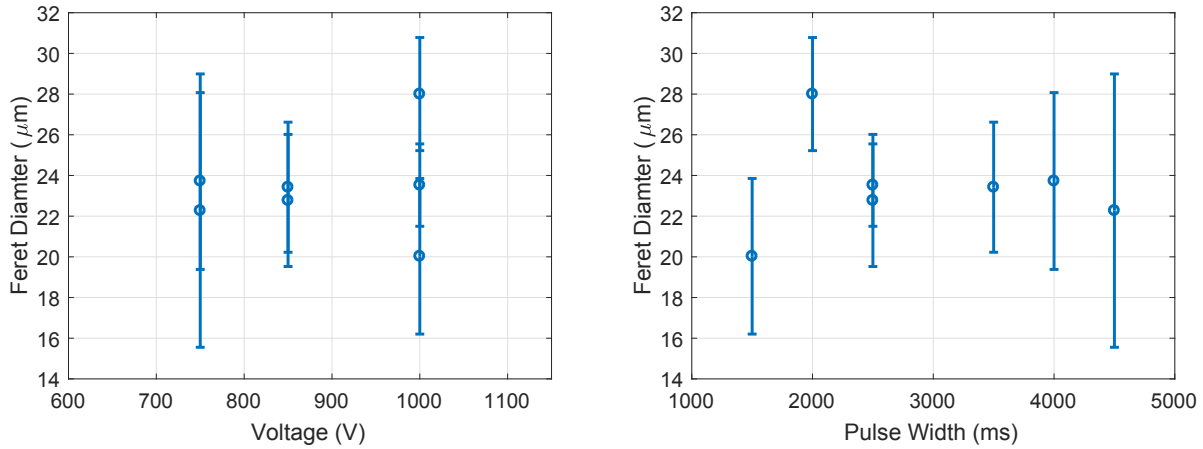


**Figure 5: Feret diameter as a function of voltage (left) and pulse width (right) for all tests.**

Further, it provides a regime in which features smaller than those observed above could be made without reducing the nozzle size as is tpyical in e-jet printing to achieve higher resolution. Figure 6 shows still images taken from a video demonstrating the intermittent jetting behavior. During the 2000 ms pulse width, seven jetting events were observed. In frames labeled $t$ =743, 908, 1238, 1321, and 1486 through 1651 ms, i.e., labeled "Jet", a sharp meniscus can be observed. While not entirely clear in the still images, primarily due to the low frame rate of the monitoring camera, a jet of material issues from the meniscus during these frames. In between the frames depicting jetting, the meniscus retracts before extending again into a sharp cone.

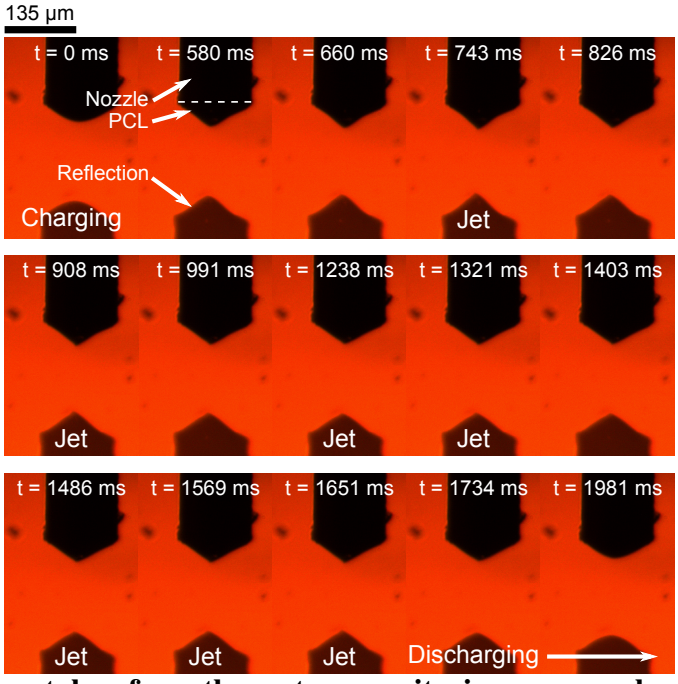


**Figure 6: Still images taken from the system monitoring camera showing evidence of an intermittent jetting mode for pure PCL.**

## Conclusion

Polycaprolactone (PCL) is an important polymer for tissue engineering applications. The typical methods for fabrication of PCL structures is through either inkjet printing or e-spinning. While both of these processes have benefits for specific applications of PCL structures, there exists a gap in fabrication methods for small patterns of fine features. E-jet printing, a process governed by the same physics as e-spinning, is a promising tool for filling this gap. Here, e-jet printing is used to demonstrate the ability to print high-resolution features using molten PCL.

In the drop-on-demand or pulse printing regime, where a pulsed voltage is applied to the printing nozzle, voltages and pulse widths ranged from 750 to 1000 V and 1500 to 4500 ms. These voltages are similar to those used in printing of other less viscous inks. However, the pulse widths are approximately two orders of magnitude greater than those typical for e-jet printing in the pulse printing regime. This property is a direct result of the limiting viscous flow for molten PCL while other ink materials are limited by the charge relaxation time. While the processing window for molten PCL is similar to that of other inks typically e-jet printed, the typical relationships between voltage and pulse width and feature volume do not appear to hold. In fact, the process appears insensitive to the magnitude of voltage applied or the duration of the applied voltage within a range. Features of approximately 20 $\mu$m were produced for all of the experimental conditions used here. This further corroborates the viscosity limiting behavior of e-jet printed molten PCL.

During initial testing, a regime was found in which intermittent jetting was observed. This is a previosuly unreported regime for PCL. While the intermittent jetting regime observed here requires large voltages (at least 1200 V), it may be a beneficial area of the process parameter space in that finer features can be fabricated without a decrease in nozzle size.

## References


[1] Ulery, B.D., Nair, L.S., Laurencin, C.T., 2011, "Biomedical Applications of Biodegradable Polymers," *Journal of Polymer Science B: Polymer Physics*, vol. 49, pp. 832-864.

[2] Scheideler, W., Chen, C.-H., 2014, "Minimum Flow Rate Scaling of Taylor Cone-Jets Issued from a Nozzle," *Applied Physics Letters*, vol. 14, pp. 024103:1-4.

[3] Ghaziof, S., Mehdikhani-Nahrkhalaji, M., 2017, "Preparation, Characterization, Mechanical Propertied and Electrical Conductivity of Novel Polycaprolactone/Multi-Wall Carbon Nanotubes Nanocomposites for Myocardial Tissue Engineering," *Acta Physica Polonica A*, vol. 131, pp. 428-431.

[4] Biresaw, G., Carriere, C.J., 2001, "Correlation between Mechanical Adhesion and Interfacial Properties of Starch/Biodegradable Polyester Blends," *Journal of Polymer Science: Part B: Polymer Physics*, vol. 39, pp. 920-930.

[5] Hedge, V.J., Gallot-Lavalee, O., Heux, L., 2016, "Dielectric Study of Polycaprolactone: A Biodegradable Polymer," *IEEE International Conference on Dielectrics*, Jul. 3-7, Montpellier, FR.

[6] Collins, R.T., Jones, J.J., Harris, M.T., Basaran, O.A., 2008, "Electrohydrodynamic Tip Streaming and Emission of Charged Drops from Liquid Cones," *Nature Physics*, vol. 4, pp. 149-154.

[7] Speranza, V., Sorrentino, A., De Santis, F., Pantani, R., 2014, "Characterization of the Polycaprolactone Melt Crystallization: Complementary Optical Microscopy, DSC, and AFM studies," *The Scientific World Journal*, vol. 2014, pp. 720157:1-9.

[8] Prabaharan, M., Mano, J.F., 2005, "Chitosan-Based Particles as Controlled Drug Delivery Systems," *Drug Delivery*, vol. 12, pp. 41-57.

[9] Jagur-Grodzinski, J., 2006, "Polymers for Tissue Engineering, Medical Devices, and Regenerative Medicine. Concise General Review of Recent Studies," *Polymers for Advanced Technologies*, vol. 17, pp. 395-418.

[10] Chen, Q.Z., Thompson, I.D., Boccaccini, A.R., 2006, "45S5 Bioglass®-Derived Glass-Ceramic Scaffolds for Tissue Engineering," *Biomaterials*, vol. 27, pp. 2414-2425.

[11] Zaiss, S., Brown, T.D., Reichert, J.C., Berner, A., 2016, "Poly($\epsilon$-caprolactone) Scaffolds Fabricated by Melt Electrospinning for Bone Tissue Engineering," *Materials*, vol. 9, pp. 232:1-15

[12] Onses, M.S., Sutanto, E., Ferreira, P.M., Alleyen, A.G., Rogers, J.A., 2015, "Mechanisms, Capabilities, and Applications of High-Resolution Electrohydrodynamic Jet Printing," *Small*, vol. 11, pp. 4237-4266.

[13] He, Y., Wildman, R.D., Tuck, C.J., Christie, S.D.R., Edmondson, S., 2016, "An Investigation of the Behavior of Solvent-based Polycaprolactone Ink for Material Jetting," *Scientific Reports*, vol. 6, pp. 20852:1-10.